PHILOSOPHICAL MAGAZINE B, 1991, VOL. 63, NO. 5, 1169–1179

On the kinetics of Ag photodissolution in As_2S_3 chalcogenide glass films: oscillatory behaviour of the reaction rate

By E. MARQUEZ†, R. JIMENEZ-GARAY†, A. ZAKERY, P. J. S. EWEN and A. E. OWEN

Department of Electrical Engineering, University of Edinburgh, Edinburgh EH9 3JL, Scotland

[*Received 28 March 1990 and accepted 14 June 1990*]

ABSTRACT

The kinetics of Ag photodissolution into As_2S_3 glass films have been investigated by monitoring the electrical resistance of the Ag layer during the process. The thickness dependence of the Ag electrical resistivity predicted by the thick-film approximation of Sondheimer's theory has been used (reasonable agreement was found), in order to obtain the curve of Ag thickness against illumination time. The thickness ranges of Ag and As_2S_3 layers studied were around 1000–1500 Å and 3000–5000 Å respectively. The main feature found is the appearance of an oscillatory behaviour of the reaction rate, with the illumination from the As_2S_3 side and wavelengths lower than a threshold value, which increased when the thicknesses of the layers were increased. In contrast, when the samples were irradiated on the Ag side, the sigmoidal kinetic curve very often reported was observed. These data could support the idea that the actinic light absorption occurs in the vicinity of the doped–undoped chalcogenide interface.

§ 1. INTRODUCTION

The photostimulated reaction between films of Ag and chalcogenide glasses, known variously as 'photodissolution' or 'photodoping', has been the object of many investigations (for example Kostyshin, Mikhailovskaya and Romanenko (1966), Janai (1981), Kluge (1987), Ewen, Zakery, Firth and Owen (1988), Kolobov, Elliott and Taguirdzhanov (1990)). Some researchers have shown the possibility of technical applications of this phenomenon, especially for preparation of inorganic photoresists for ultra-high-resolution lithography (Chen and Tai 1980, Yoshikawa, Ochi and Mizushima 1980, Firth, Ewen and Owen 1985a, Firth, Ewen, Owen and Huntley 1985b) and infrared grating fabrication (Zakery, Slinger, Ewen, Firth and Owen 1988). However, the actual mechanism of photodissolution still remains unclear. In particular, there is uncertainty concerning where the actinic radiation is absorbed and what is the photodissolution rate-limiting step. In this paper, some new experimental data for clarifying the kinetics of the photodoping process of Ag into amorphous As_2S_3 (*a*–As_2S_3) are reported. From these results it is possible to address the above-mentioned fundamental questions. Specifically, the photodissolution rate of the metal has been monitored by the electrical resistance measurement technique described elsewhere (Goldschmidt and Rudman 1976) and, principally, samples with thick Ag layers have

† Permanent address: Departamento de Estructura y Propiedades de los Materiales, Facultad de Ciencias, Universidad de Cadiz, ap. 40 11510 Puerto Real, Cadiz, Spain.

been investigated. The main kinetic characteristic that will be reported is the appearance of an oscillatory behaviour of the reaction rate (OBRR), when the Ag/As_2S_3 system was illuminated from the chalcogenide side of the sample.

§ 2. Experimental details

Films of a–As_2S_3 were prepared by thermal evaporation, in a vacuum of about 10^{-5} Torr; Ag metal was pre- or post-deposited also by evaporation (Ewen *et al.* 1988). The As_2S_3 evaporation source was powdered melt-quenched glass and the metal source was fragments of Ag wire. The sample configuration is illustrated in fig. 1. The substrate was a glass microscope slide, each slide containing ten silver strips. The dimensions of the silver strips and the chalcogenide glass film were approximately 1 mm × 2 cm and 1·3 cm × 6·5 cm respectively. In order to generate this pattern, two masks were used during the evaporation. The deposited thicknesses were determined by means of a quartz oscillator thickness monitor which had been calibrated against a Sloan Dektak IIA surface profiler. The As_2S_3 and Ag layer thicknesses ranged mostly between around 3000 and 5000 Å and around 1000 and 1500 Å respectively. The ratio of the thicknesses of Ag to As_2S_3 layers selected was slightly lower than 1 to 3, in order to make sure that the silver strip was completely exhausted (Firth *et al.* 1985a). The electrical contacts with the silver strip were made with tungsten probes with springs and an x–y–z micromanipulator attached (fig. 1). With this arrangement a gentle contact pressure and, consequently, a stable electrical resistance, essential in this experiment, was achieved. The two-terminal resistance measurements were made using a Keithley 195 programmable digital multimeter (DMM), microcomputer controlled via an IEEE-488 interface, so that the data could be logged and processed

Fig. 1

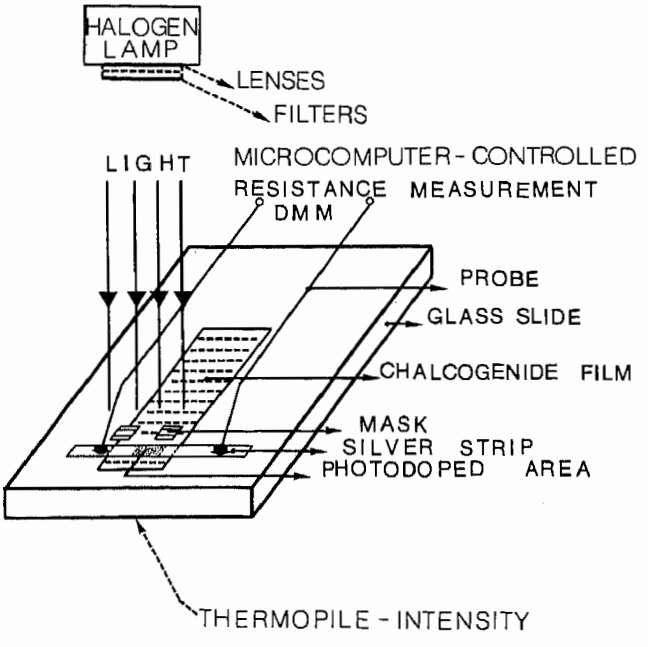

The experimental set-up for measuring the electrical resistance of the silver layer as a function of irradiation time, during the Ag photodissolution effect.

automatically. To check that Joule self-heating or electromigration effects did not occur significantly, some results were also obtained using a 1 μA constant current method for measuring the resistance. The results were similar in both cases and the DMM has the advantage of offering a higher signal-to-noise ratio (this instrument has a $10^{-4}\,\Omega$ sensitivity). The light irradiation of the sample was by means of a 150 W W–halogen lamp with light guide and heat filter. The wavelength of the radiation was controlled by suitable optical filters, and the light intensity (which was measured with a thermopile) was modified by varying the distance between the sample and the outlet of the light guide. Care was taken with the uniformity of the light beam over the illuminated area of the sample. All measurements reported here were performed at room temperature.

§3. Relationship between Ag thickness and resistance increase

The measurement of the Ag layer resistance continuously during illumination has enabled the change in Ag layer thickness to be determined also continuously, based on the equation

$$\Delta R(d) = (l/w)[\rho(d)/d - \rho(d_0)/d_0], \tag{1}$$

where l is the length (in the direction of the current) of the zone of the silver strip to be illuminated and d its thickness (during the reaction), and w and d_0 are the width and initial thickness of the silver strip; ΔR is the increase in the resistance and ρ is the electrical resistivity of Ag. The expression for the electrical resistance in the present configuration, $R = R_c + \rho l'/wd_0$, l' being the interprobe distance, has two terms corresponding to the contact resistance and the resistance of the Ag layer. Using the latter equation and measuring the resistance for several widths and interprobe distances, the resistivity of Ag was calculated (a good fit to a linear relationship between the resistance and aspect ratio l'/w was generally found).

Furthermore, the thickness dependence of resistivity predicted by the thick-film approximation of Sondheimer's theory (for example, Sondheimer (1952), Berry, Hall and Harris (1968), Larson (1971)), for the most realistic case of inelastic scattering at the film boundaries is

$$\rho(d) = (mv_F/ne^2)(1/\lambda_\infty + 3/8d) = \rho_\infty(1 + 3\lambda_\infty/8d), \tag{2}$$

where m, v_F, n and e are the electron mass, the Fermi speed, the density of electrons and the electron charge; ρ_∞ and λ_∞ are the resistivity and mean free path of the electrons corresponding to infinite film thickness (λ_∞ includes each of the effects that limit the mean free path of the electrons, such as phonons, impurities, defects and grain boundaries). Good agreement between this theory and the experimental results, using Ag evaporated films, in the thickness range from about 100 to 2000 Å, has been obtained (Reynolds and Stilwell 1952). The significant feature of the sample preparation procedure used in that investigation was the high evaporation rate employed (about 500 Å s^{-1} or higher). The value of the mean free path found was 520 Å and the Ag bulk resistivity value used was 1·62 $\mu\Omega$ cm. In the present study, slightly higher values of the resistivity have been obtained because of the lower deposition rate achieved, around 100 Å s^{-1}. The value of the electrical resistivity clearly depends on the deposition rate as a consequence of the strong influence of the evaporation rate on the final structure of the film (table 1 shows some typical results). In addition, it is assumed that the photodissolution process is also influenced by the structural characteristics of the Ag film and, for this reason, the Ag resistivity provides useful preliminary

Table 1. Electrical resistivity of Ag films 1300 Å thick prepared with different deposition rates and the ratio of these experimental values to the resistivity predicted by eqn. (2) (with $\rho_\infty = 1{\cdot}62\ \mu\Omega\,\text{cm}$ and $\lambda_\infty = 520$ Å), $1{\cdot}86\ \mu\Omega\,\text{cm}$.

Deposition rate (Å s^{-1})	$\rho_{\text{experimental}}$ ($\mu\Omega\,\text{cm}$)	Resistivity ratio
10	5·40	2·90
50	2·57	1·38
100	2·05	1·10

information. On the other hand, as a result of the difference between the values of resistivity reported by Reynolds and Stilwell and those obtained in this investigation, it was necessary to recalculate the parameters ρ_∞ and λ_∞ from the silver resistivity found. In the case of $d_0 = 1300$ Å with $\rho = 2{\cdot}05\ \mu\Omega\,\text{cm}$, $\lambda_\infty = 466$ Å and $\rho_\infty = 1{\cdot}81\ \mu\Omega\,\text{cm}$ (the effective mean free paths were similar for the majority of the Ag film thicknesses analysed). It should be taken into account that $\lambda_\infty^{-1} = \lambda_{\text{ph}}^{-1} + \lambda_{\text{imp}}^{-1} + \lambda_{\text{def}}^{-1} + \lambda_{\text{bdy}}^{-1} + \ldots$, that is each of the effects that limit the mean free path may be considered to act independently of the others (only the supposedly main contributions have been indicated explicitly here). Thus it is assumed that eqn. (2), with the readjusted parameters, accounts for the Ag resistivity increase as a consequence of the Ag thickness reduction during the photodoping process with reasonable accuracy. (If, as suggested in § 4, the Ag reacts preferentially at grain boundaries to produce an uneven interface, then the Ag thickness d will be an average value.) Finally, combining eqns. (1) and (2), the Ag thickness as a function of the resistance increase is deduced:

$$d(\Delta R) = [d_0/\alpha(\Delta R)]\{1 - [1 + 4\alpha(\Delta R)\beta]^{1/2}\}, \tag{3}$$

where the dimensionless magnitudes α and β are given by

$$\alpha(\Delta R) = 1 + \beta + \Delta R w d_0/\rho_\infty l, \quad \beta = 3\lambda_\infty/8d_0.$$

§ 4. Results and discussion

Some significant experimental results concerning photodissolution in the Ag/As_2S_3 system will now be presented. Firstly, the electrical resistance as a function of illumination time, for two values of the exciting light intensity, 1·10 and 4·30 mW cm^{-2}, is shown in fig. 2. These results correspond to samples whose initial Ag and chalcogenide glass thicknesses are approximately 1300 and 4700 Å respectively. Unfiltered light was used in this particular case and the illumination took place from the chalcogenide side of the sample. The intensity range studied in this work, when 'white' light was employed, was about 1–10 mW cm^{-2}. The outstanding feature of these typical curves plotted in fig. 2 is that there are several changes in the sign of the quantity d^2R/dt^2 during the photodissolution process; in the case of the lower intensity there are three inflection points and with the higher intensity there are only two. Secondly, in fig. 3, the electrical resistance data converted by means of eqn. (3) to Ag thickness, as a function of exposure time, are shown. Both time dependences show that the reaction speeds initially increase and then decrease, repeating this oscillatory behaviour once more during the process. In addition, the corresponding photodoping rate derived by the Gregory–Newton numerical differentiation method against the normalized quantity, fraction of Ag reacted, for both light intensities is plotted in the same figure. Two peaks are observed in these curves and a characteristic of them is that the

Fig. 2

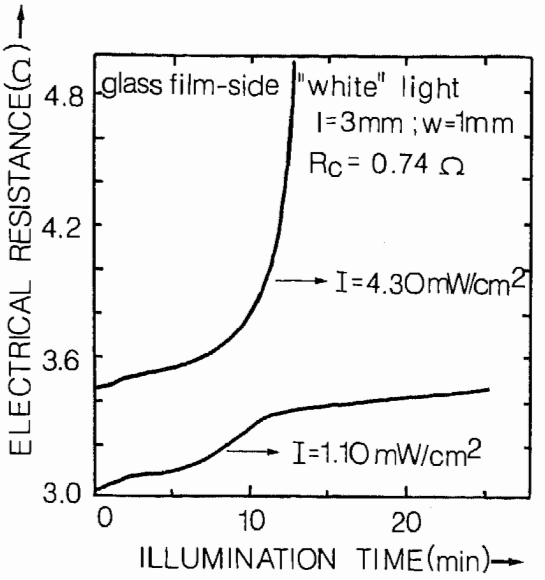

The Ag electrical resistance against exposure time curve corresponding to two light intensities (unfiltered light was used). The dimensions l and w of the illuminated area of the sample and the average contact resistance in the present measurements are indicated in the figure.

difference between the reaction rates at the first maximum is considerably less than at the second maximum; moreover, the difference between the positions of the first maxima is also insignificant in comparison with that existing between the positions of the second maxima (table 2). Furthermore, the plots of Ag thickness against exposure dose (light intensity multiplied by exposure time) for the different power densities studied do not follow a common curve, so that the OBRR does not obey the reciprocity law, that is the interchangeability of light intensity and irradiation time. To illustrate this characteristic, for an exposure dose of $1\,J\,cm^{-2}$, light intensities of 1·1, 4·3 and $8{\cdot}5\,mW\,cm^{-2}$ yield Ag thicknesses of 540, 970 and 1010 Å respectively. On the other hand, when this particular type of sample was irradiated from the chalcogenide side using filtered light with different wavelengths, whose values were 400, 525, 570 and 650 nm respectively, the kinetic characteristics observed with unfiltered light continued to appear in the case of the first three wavelengths; however, for the longest wavelength of 650 nm no oscillation in the reaction rate was observed. The latter experimental finding is of fundamental importance in order to discover the origin of the phenomenon. Other experimental results belonging to samples with different initial Ag and As_2S_3 thicknesses, $d_0(Ag) \approx 1200$ Å and $d_0(As_2S_3) \approx 4100$ Å, with the illumination from the chalcogenide side, are plotted in fig. 4. These curves of electrical resistance against illumination time have been obtained using 525 nm green light (fig. 4 (*a*)) and unfiltered light (fig. 4 (*b*)); the inflection points of these curves, which give rise to OBRR, may be seen more clearly in this figure (these are marked in the plots with arrows).

In contrast, when the samples investigated were illuminated on the Ag side their behaviour was different; a three-stage kinetic curve was obtained, similar to that very often reported in the literature (for example Goldschmidt and Rudman (1976), Yaji and

Fig. 3

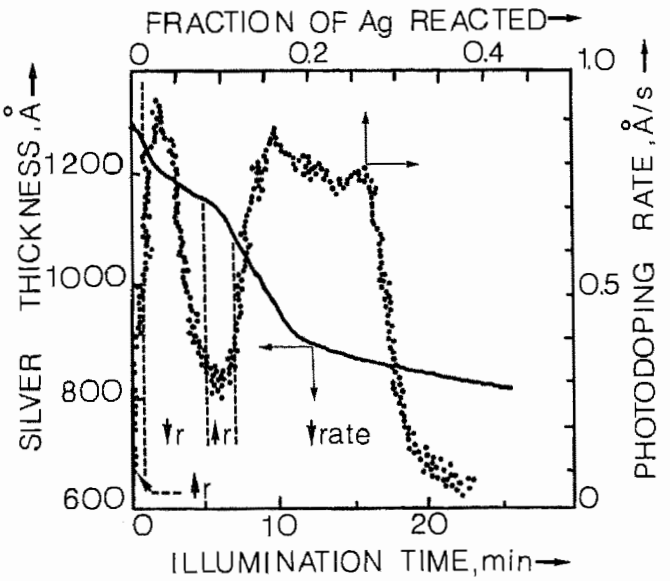

(*a*)

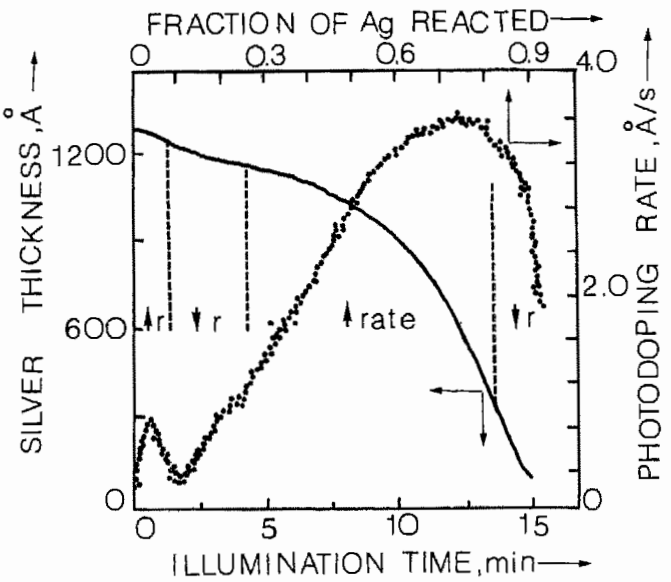

(*b*)

Variation in Ag thickness as a function of illumination time and variation in the photodissolution rate as a function of fraction of Ag reacted, as derived from the Ag resistance against exposure time curves plotted in fig. 2: (*a*) 1·10 mW cm^{-2}; (*b*) 4·30 mW cm^{-2}. In this figure are also shown the distinct stages of the process in which $dr/dt > 0$ or $dr/dt < 0$. The inflection points of these kinetic curves, with $dr/dt = 0$, have been deduced from the associated photodoping rate against normalized Ag thickness plots.

Table 2. Values of the photodissolution rate and the percentage of Ag layer photodoped, at the first and second maximum of the curves showing the variation in the rate during the process plotted in fig. 3.

Unfiltered light power density ($mW\,cm^{-2}$)	First-maximum photodoping rate ($Å\,s^{-1}$)	Second-maximum photodoping rate ($Å\,s^{-1}$)	First-maximum position (%)	Second-maximum position (%)
1·10	0·93	0·87	2·5	16
4·30	0·81	3·59	3·0	73

Fig. 4

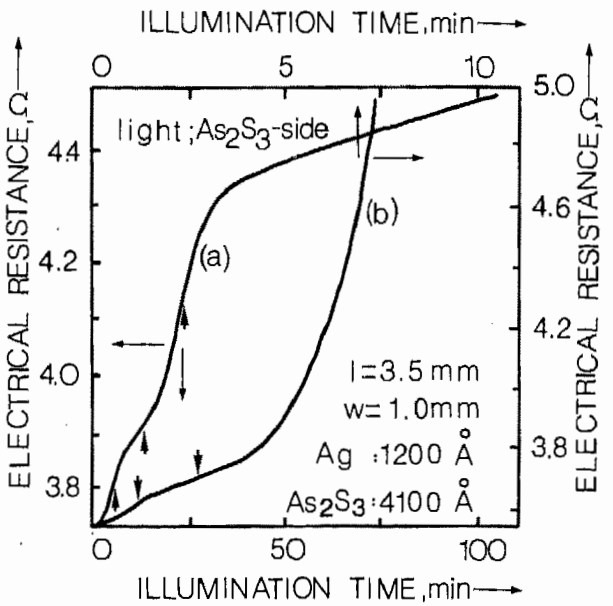

Time dependence of Ag resistance for (*a*) 525 nm green light, with $I = 1{\cdot}50\,mW\,cm^{-2}$, and (*b*) unfiltered light, with $I = 8{\cdot}10\,mW\,cm^{-2}$. The thicknesses of the two layers and the length and the width of the irradiated region are also indicated in the figure.

Kurita (1983), Konan, Galibert and Calas (1988)), with a sigmoidal form, that is with an acceleratory period (the so-called induction period), a linear stage and, finally, a deceleratory step. The linear stage is usually interpreted as a chemical-reaction-limited process and part of the deceleratory period may be presumably due to a diffusion process (the movement of the interface between the photodoped and the Ag layers being limited by the motion of Ag^+ ions through the photodoped layer), since a square root time dependence has been seen after the linear stage. Finally, the violation of the parabolic law observed at the end of the photodoping process could be caused by the reduction in the amount of light reaching the reaction interface, due to absorption in the highly absorbing photodoped layer (see § 5); this would produce an additional decrease in the reaction rate. As a typical result (fig. 5), an induction period of 23·5 min and a photodoping rate corresponding to the linear stage of $0{\cdot}15\,Å\,s^{-1}$ was found for a

sample with an initial Ag thickness of approximately 1000 Å and an initial As_2S_3 thickness of approximately 3100 Å, using 400 nm ultraviolet light and a photon flux density of $1{\cdot}13 \times 10^{15}$ photons $cm^{-2}\,s^{-1}$. Moreover, the part of the deceleratory period in which the thickness of the reacted Ag layer is proportional to $t^{1/2}$ is displayed in fig. 5 (the parabolic rate constant derived from this interval was $1{\cdot}5 \times 10^{-7}$ cm $s^{-1/2}$). When this type of sample was illuminated from the As_2S_3 side employing filtered light with the above-mentioned distinct wavelengths, the OBRR shown in fig. 3 disappeared for

Fig. 5

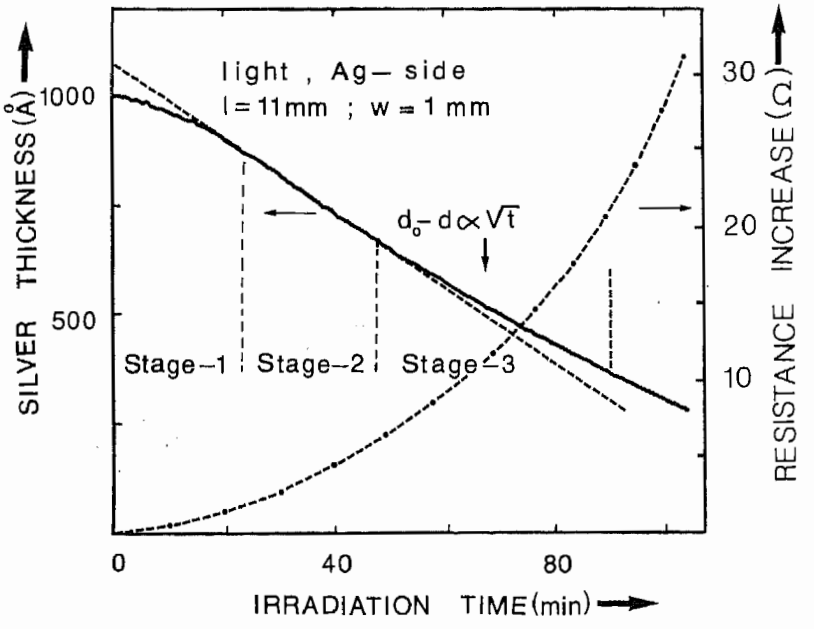

Decrease in Ag thickness during irradiation, with 400 nm ultraviolet light incident on the Ag side of the sample, the initial As_2S_3 layer thickness being around 3100 Å ($I = 0{\cdot}56$ mW cm^{-2}). The curve of Ag resistance increase against illumination time is also plotted. The dimensions of the illuminated zone are also indicated in the figure.

Table 3. Spectral dependence of the linear stage photodoping rate ($I = 1{\cdot}4$ mW cm^{-2}). The oscillations observed with $\lambda = 400$ nm appeared after the initial linear step, and therefore it was possible to derive the photodoping rate associated with this period. Other results (Zakery 1990) relating to a–As_2S_3, obtained by optical reflectivity measurements (this technique is described by Ewen *et al.* (1988)) are consistent with those found by electrical resistance measurements. From the former data, it has been determined that the photodissolution rate decreases very sharply for $\lambda \gtrsim 500$ nm.

Light wavelength (nm)	Photon energy (eV)	Linear stage photodoping rate (Å s^{-1})	Photodoping rate normalized to r(525 nm)
400	3·11	1·14	0·49
525	2·37	2·34	1·00
570	2·18	1·06	0·45
650	1·91	0·25	0·11

all wavelengths except in the shortest wavelength of 400 nm; the kinetic curve when the oscillations disappeared, with the light incident on the As_2S_3 side, was analogous to that displayed in fig. 5, except that there was no induction period or it was too short to be measured, such as has been seen in the OBRR plots (some values of the linear stage photodoping rate are shown in table 3). The non-appearance of OBRR when the light is incident on the Ag side of the sample has also been observed in very thin films. As a representative example, in a sample with $d_0(Ag) \approx 200$ Å and $d_0(As_2S_3) \approx 700$ Å, the S-shaped kinetic curve was again found, and the induction period and linear stage photodoping rate were 46 s and 0·40 Å s^{-1}. These results were obtained with $\lambda = 570$ nm and $I = 1{\cdot}45$ mW cm^{-2}. The exposure time in order to photodissolve completely the illuminated zone of the silver strip was 13 min. This exposure time is determined from the electrical resistance against irradiation time curve; when the Ag layer is exhausted, the measured resistance is commonly about several megohms ($R = 2{\cdot}5$ MΩ in the example under consideration) and this value corresponds to the doped layer resistance (the ratio of the resistance of the undoped area to that of the Ag-doped area was 7×10^4 in this particular case). Note that the doped-layer resistance is around six orders of magnitude higher than the initial Ag resistance, justifying the correctness of the basic assumption of the electrical method used for monitoring the kinetics of the phenomenon, namely $\rho_{Ag} \ll \rho_{As_2S_3}$ and ρ_{Ag/As_2S_3}.

In summary, from the experimental data of the present study the following features regarding the kinetics of the effect may be deduced.

(1) The structure of the kinetic curve showing OBRR depends clearly on the exciting power density (reciprocity behaviour was not observed).
(2) The existence of OBRR depends on whether the light passes through the Ag polycrystalline layer first, or whether the light passes through the chalcogenide glass layer first.
(3) The role of the light wavelength for finding the OBRR was crucial, since in the cases investigated when the wavelength was increased this disappeared, depending on the initial thicknesses of the two layers (note that most of the initial Ag thicknesses used have been higher than those employed in the majority of the kinetic studies by electrical resistance measurement and other techniques, which used films of thicknesses 1000 Å or less).

Analogous results for the Ag photodoping of a–As_2S_3 with the irradiation on the chalcogenide side have been reported (Arai *et al.* 1989), using annealed and photodarkened samples in this study. It has been argued that the time dependence of the reaction shows a clear two-stage behaviour. During the initial stage of the irradiation, the Ag–doped-chalcogenide interface shift exceeds the decrease in Ag thickness, while in the second stage the process is inverted. The spectral dependence of the phenomenon was also studied and suggested that only photons with energy higher than the As_2S_3 optical bandgap, $E_g = 2{\cdot}33$ eV, are able to give rise to the second stage of the process. From these results and Rutherford backscattering data, it was concluded that the mechanism responsible for the first stage is different from that for the second stage.

A corresponding investigation in a–$GeSe_2$ has also reported similar behaviour (Rennie 1986, Rennie and Elliott 1987). Small oscillations superimposed on the Ag thickness against illumination time curves, again when the light exposure was from the chalcogenide side of the sample, were also observed. Such oscillations, together with those found in the photodoping rate as a function of the initial Ag thickness, were

interpreted as an optical interference process occurring in this multilayer optical system; their presence allows the possibility of determining where in the sample the absorbed light leads to reaction. From calculations of the light intensity at various points of the multilayer structure, it was concluded that the light stimulating metal photodoping is absorbed at the photodoped–undoped chalcogenide interface. Another conclusion to be drawn from this analysis in relation to the interpretation of the present results is that the number of oscillations in the photodissolution rate during the process decreases considerably when the light wavelength is increased, as would be expected if this were an interference effect.

Considering only the shape of the plots of photoreaction rate against the fraction of Ag reacted shown in fig. 3, it would be plausible to argue that the phenomenon consists of two stages with distinct mechanisms, such as has been suggested for annealed and photodarkened a–As_2S_3, the second step being much more sensitive to the value of the incident power density. However, since the oscillations disappeared when the radiation wavelength was increased (when d_0(Ag) and $d_0(As_2S_3)$ were increased, the threshold wavelength at which the OBRR disappeared was also increased), it seems reasonable to think that, on the contrary, these observations for a$-As_2S_3$ may be a consequence of an optical interference effect, which would give rise to oscillatory variations of the actinic light intensity. Furthermore, although the above-mentioned calculations of intensity also predict the OBRR with illumination from the Ag side, the polycrystalline nature of the as-deposited Ag film may give rise to a preferential reaction at the grain boundaries (due presumably to increased stress and defect concentration generally found in these regions), producing an uneven Ag–photodoped chalcogenide interface (S. R. Elliott 1989, private communication) and therefore a strong reduction in the interference effect. It could explain the non-appearance of OBRR when the light passes through the Ag layer first. On the other hand, the OBRR observed with white light (broad-band illumination) could occur because of the spectral dependence of the photodoping rate (table 3) and the spectral irradiance distribution of the W–halogen lamp used. This relative spectral energy increases monotonically from around 300 nm, being 12% at 400 nm, 36% at 500 nm and 60% at 600 nm. From the combination of these two spectral dependences may result a dominant contribution of a reasonably narrow wavelength range, which would justify the existence of OBRR even with unfiltered light. Moreover, the peak positions of the OBRR curves could be affected by the value of the incident light intensity (the corresponding interference pattern would not depend on the power density), because the photodissolution process is supposedly controlled, not only by the chemical reaction at the doped–undoped interface, but also by the diffusion of Ag^+ ions through the doped layer.

§ 5. Concluding remarks

A comprehensive study of the optical constants (refractive index and absorption coefficient) of undoped and Ag-doped As–S glasses is currently being carried out in this laboratory (Zakery *et al.* 1988, Zakery, Zekak, Ewen, Slinger and Owen 1989) which will enable a computer simulation of this effect to be carried out. The calculations required for the light amplitudes at the two interfaces of the sample will be carried out by a matrix method using the Fresnel coefficients described by Heavens (1955), which is a more convenient technique. The Fresnel coefficients depend on the quantities Δn and $\Delta\alpha$, the difference between the refractive indices and absorption coefficients of the doped and undoped material. As a representative instance of results found in the above study of the optical constants, for the composition $As_{30}S_{70}$ and the most heavily doped

sample ($d_0(As_{30}S_{70}) \approx 5000$ Å and $d_0(Ag) \approx 1500$ Å), which contained approximately 27 at.% Ag, $\Delta n > 0{\cdot}5$ over the wavelength range 500–2000 nm and the values of α of undoped and doped films at, for example, 514 nm are $4{\cdot}5 \times 10^2$ and $6{\cdot}9 \times 10^4$ cm^{-1} respectively, the ratio of these two values of α in the visible spectrum being approximately 10^2. The results of modelling the kinetics of the process by the procedure proposed could strongly support the explanation of OBRR in a–As_2S_3 based on the variations in the intensity at the doped–undoped chalcogenide interface. In other words, the actinic light absorption would take place in that region of the multilayer system (it should be noted that according to the absorption coefficients the photodoped zone is significantly more absorbing), as has also been deduced from the experiments of the lateral migration of Ag in As–S films in contact with a conducting substrate (Owen, Firth and Ewen 1985) and other recent experiments (Kolobov *et al.* 1990).

Acknowledgments

The authors are grateful to Mr J. Wilson and Mr A. Zekak for their helpful cooperation during this investigation and would like to thank Dr S. R. Elliott for valuable discussions relating to this work. One of us (E.M.) is also grateful to the Spanish Ministry of Education and Science for the concession of a research grant.

References

Arai, T., Wakayama, Y., Kudo, H., Kishimoto, T., Lee, J., Ogawa, T., Onari, S., 1989, *J. non-crystalline Solids*, **114**, 40.

Berry, R. W., Hall, P. M., and Harris, M. T., 1968, *Thin Film Technology* (Princeton, New Jersey: Van Nostrand).

Chen, C. H., and Tai, K. L., 1980, *Appl. Phys. Lett.*, **37**, 605.

Ewen, P. J. S., Zakery, A., Firth, A. P., and Owen, A. E., 1988, *Phil. Mag.* B, **57**, 1.

Firth, A. P., Ewen, P. J. S., and Owen, A. E., 1985a, *J. non-crystalline Solids*, **77–78**, 1153.

Firth, A. P., Ewen, P. J. S., Owen, A. E., and Huntley, C. M., 1985b, *Advances in Resist Technology and Processing II*, Proc. SPIE, Vol. 539, edited by L. F. Thompson (Bellingham, Washington: SPIE), p. 160.

Goldschmidt, D., and Rudman, P. S., 1976, *J. non-crystalline Solids*, **22**, 229.

Heavens, O. S., 1955, *Optical Properties of Thin Solid Films* (London: Butterworth).

Janai, M., 1981, *Phys. Rev. Lett.*, **47**, 726.

Kluge, G., 1987, *Phys. Stat. sol.*, **101**, 105.

Kolobov, A. V., Elliott, S. R., and Taguirdzhanov, M. A., 1990, *Phil. Mag.* B, **61**, 857.

Konan, K., Galibert, G., and Calas, J., 1988, *Phys. Stat.* sol., **107**, 273.

Kostyshin, M. T., Mikhailovskaya, E. V., Romanenko, P. F., 1966, *Fizika tverd. Tela*, **9**, 571.

Larson, D. C., 1971, *Physics of Thin Films*, edited by G. Hass and R. E. Thun (London: Academic Press), p. 81.

Owen, A. E., Firth, A. P., and Ewen, P. J. S., 1985, *Phil. Mag.* B, **52**, 347.

Rennie, J. H. S., 1986, Ph.D. Thesis, Jesus College, Cambridge.

Rennie, J. H. S., and Elliott, S. R., 1987, *J. non-crystalline Solids*, **97–98**, 1239.

Reynolds, F. W., and Stilwell, G. R., 1952, *Phys. Rev.*, **88**, 418.

Sondheimer, E. H., 1952, *Adv. Phys.*, **1**, 1.

Yaji, T., and Kurita, S., 1983, *J. appl. Phys.*, **54**, 647.

Yoshikawa, A., Ochi, O., and Mizushima, Y., 1980, *Appl. Phys. Lett.*, **36**, 107.

Zakery, A., 1990 (private communication).

Zakery, A., Slinger, C. W., Ewen, P. J. S., Firth, A. P., and Owen, A. E., 1988, *J. Phys.* D, **21**, S78.

Zakery, A., Zekak, A., Ewen, P. J. S., Slinger, C. W., and Owen, A. E., 1989, *J. non-crystalline Solids*, **114**, 109.